LA-UR -83-3042

CONF-831015--11

Los Alamos National Laboratory is operated by the University of California for the United States Department of Energy under contract W-7405-ENG-36

TITLE: NANOSECOND IMAGE-SHUTTERING STUDIES AT LOS ALAMOS NATIONAL LABORATORY

LA-UR--83-3042

DE84 001733

AUTHOR(S): G. J. Yates, P-15
N. S. King, P-15
S. A. Jaramillo, P-15
B. W. Noel, WX-10
P. L. Gobby, MST-6
I. Aeby, EG&G, Santa Barbara
J. L. Detch, EG&G, Santa Barbara

SUBMITTED TO. IEEE 1983 Nuclear Science Symp.
San Francisco, CA
October 19-21, 1983

DISCLAIMER

Los Alamos
Los Alamos National Laboratory
Los Alamos, New Mexico 87545

FORM NO 836 R4
ST NO 2629 5/81

NANOSECOND IMAGE-SHUTTERING STUDIES AT LOS ALAMOS NATIONAL LABORATORY

G.J. Yates, P.S.P. King, S.A. Jaramillo, B.W. Noel, P.L. Gobby
Physics Division, University of California, Los Alamos National Laboratory
Group P-15, Mail Stop D406, P.O. Box 1663, Los Alamos, New Mexico 87545

and

I. Aeby and J.L. Deutch
EG&G Inc. Santa Barbara Operations
130 Robin Hill Road, P.O. Box 98, Goleta, California 93017

Abstract-Experimental results comparing gated imaging capabilities of proximity-focused microchannel-plate intensifiers and electrostatically-focused silicon-intensified-target vidicons are presented. A brief summary of previous response data obtained from several standard and modified versions of both image sensors and current efforts on (1) sector gating of segmented photocathodes (2) pre-pulsing of photocathodes with infrared light to increase conductivity and (3) gate pulse injection techniques are discussed. Segmented photocathodes increased gating speed by simultaneous turn-on of individual sectors whereas preliminary analyses indicate no improvements from infrared illumination.

I. Introduction

Experiments have been conducted that identify the imaging capabilities of two different types of nanosecond-to-subnanosecond optical shutter tubes used for recording time resolved two dimensional images. We reported [1] typical temporal shuttering sequences, gating speeds, optical and electrical gate-width correlations, gain, dynamic ranges, shuttering efficiencies, and resolution for conventional and modified ITT F4111 proximity-focused microchannel-plate intensifier tubes (MCPTs). These data were compared later [2,3] with similar data obtained for ITT F4112 MCPTs and for GE-Z7821G electrostatically-focused silicon-intensified target vidicons (SITVs) recently developed jointly by General Electric and Los Alamos National Laboratory.

This paper briefly describes fast shutter design criteria, then summarizes our major experimental observations with updated measurements of dynamic shutter ratio and reciprocity for the ITT and GE units as well as for Varo 5772-310 type II MCPTs. We also report current research on (1) sector gating of segmented photocathodes to increase gating speed by effectively reducing the photo surface area (2) priming of the photocathode with pulsed infrared illumination to reduce resistivity by dynamically-induced conductivity during gate time and (3) gate driving techniques including multipoint driving and impedance matching between pulse generator and shutter gates.

II. Fast Shutter Design Criteria

Physical parameters crucial to gating speed include the photocathode-to-gate grid spacing for SITVs (or the photocathode-to-MCP input spacing for MCPTs) and the photocathode and adjacent surface resistivities. These control the effective capacitance and resistance of the gate interface.

We have studied [3-5] the gating properties of such interfaces using a model which examines the gate voltage propagation (across the interface) problem as a distributed RC network with wave propagation characteristics similar to those of a radial transmission line. This theory predicts gating speeds and shuttering patterns which are in good agreement with our experimental data [1-3] for propagation velocities $\leq 10\%$ the speed of light. In this time range (gate times of the order of 300 to 400ps or longer) we find the turn on time τ, (for peak gate voltage amplitude to appear at the pc center) to be predicted [4] by

$$\tau = \frac{R_0 C_1 a}{\pi}$$

where R_0 is the combined sheet resistance of the two gate interface surfaces, C_1 is the capacitance per unit area of the gate interface, and a is pc area.

The SITV was designed for fast shuttering by providing a lower gate-interface capacitance than that obtainable from similar sized MCPTs. The electrostatic-focused design permits locating the gate grid at greater distances (25 to 75 mils in the 7821G) from the photocathode than typical photocathode-to-microchannel plate spacings (from 7 to 10 mils in the F4111 and F4112) required for proximity focusing of MCPTs. The lumped gate capacitance for 25 mm diameter photocathode SITVs with 50-mil gate gaps is $\sim$ 3.5 pf. For 18 and 25 mm diameter MCPTs this capacitance is about 10 and 19 pf respectively. This does not include the additional perimeter capacitance existing in both designs because that capacitance only affects the reaction time from application of the gate voltage to start of the optical gate.

Both tube types use electrically conductive and optically transparent substrates to effectively lower the high resistance ($\sim 10^{10}$ to 10^{11} Ω/square) of the S-20 photocathodes. The thin film substrates used in the present designs are nickel for SITVs and chromium for MCPTs. Measurement of optical transmission vs sheet resistance for nickel were made at GE by simultaneous evaporation of the nickel on a one square inch sample plate and on the SITV fiber optic faceplate prior to formation of its photocathode. Similar measurements were made at ITT during photocathode formation by in situ monitoring of transmission and sheet resistance of a sample photocathode processed concurrently with the photocathode to be used on the MCPT. The test results are in Table I. Our nickel data are in good agreement (within 2%) with measurements made at EG&G [6] but our chromium data are only in fair agreement (within 10%) and are being repeated with better control of the radii of the two circles used in calculating the sheet resistance of the annulus containing the test photocathode substrate.

TABLE I. Photocathode substrate properties

Material	Sheet Resistance (Ω/□)	Relative Transmission %
Nickel	100	50
Nickel	71	44
Nickel	50	36
Nickel	33	30
Nickel	20	13
Nickel	11	14
Chromium	1.9×10^3	61
Chromium	0.84×10^3	61

For 18 mm diameter MCPTs $R_0 \approx 10^3$ Ω/square, $C_1 \approx 4\times10^{-14}$ F/mm, $a \approx 254$ mm^2 which gives $\tau \approx 3.24$ ns. For the 25 mm diameter MCPTs with $a \approx 491$ mm^2, $\tau \approx 6.25$ ns. However, for 25-mm-diameter SITVs $R_0 \approx 100\Omega$/square, $C_1 \approx 7\times10^{-15}$ F/mm^2, and $a \approx 491$ mm^2 which gives an unrealistically small value of 109 ps for τ. We are reviewing possible modifications to our radial model to make it applicable for propagation velocities approaching the speed of light. We are also analysing the gate interface [3] by treating it as a high frequency waveguide.

Our equation for τ shows that the propagation time of the gate pulse is directly proportional to the area it must traverse. The photocathode area, however, must remain as large as possible to provide adequate input area for imaging. Two attractive possibilities for reducing area were considered. One idea was to divide the area into four quadrants with insulating strips to provide smaller areas and also independent gating of individual segments. Preliminary designs for such a SITV have been completed but none have been built because of anticipated manufacturing complexities. The second approach considered was to form the quadrants with a conductive cross. Several SITVs and MCPTs have been fabricated in this manner.

To predict the gate response of such tubes a diffusion wave equation was developed in generalized coordinates and applied to the problem of sector-gated MCPTs with cylindrical geometry. An open form solution in terms of Bessel functions has been found. We expect to apply the same theory using spherical coordinates to sector-gated SITVs with the resulting solution appearing as a summation over a set of spherical harmonic functions. A report describing these calculations and predicted gating characteristics is in progress.

III. Summary of Comparative Responses

Neither tube type has superior performance in all areas investigated. The MCPTs have superior sensitivity, gain, and shuttering efficiency. The SITVs have superior optical gating speed, resolution, and for times shorter than ~ 5ns, they exhibit better correlation between electrical and optical gate widths. The dynamic range is determined by the vidicon which performs the read-out function (as an integral part of the SITV and fiber-optically coupled to the MCPT) for both.

All MCPTs measured show the familiar "iris" turn-on behavior where the perimeter transmits first as the gate voltage propagates radially inward. Turn-off for MCPTs can start either from the perimeter inward, the center outward, or both. No iris behavior has been observed for SITVs with nickel substrates, although it was noted on units with straight S-20 photocathodes. Turn-on shows nearly uniform initiation of transmission with increased gate time giving increased signal associated with the Gaussian gate voltage. Several shutter sequences are shown in Fig. 1. Typical gate times, resolution and shutter ratios are found in Table II.

IV. Reciprocity and Resolution vs Light Pulse Width

(a) Resolution The primary use of gated tubes is to provide an optical shutter for ≈ 1.5 to 5ns. The incident flux can have variable width from ≈ 200ps to greater than or equal to the optical gate width. Because of this uncertainty, and because our calculations on deflection defocusing for SITVs [3] indicate that image focus varies with charge density in the SIT, we measured resolution as a function only of input light pulse width in the range from 150 ps to 2.5ns.

The system used is shown in Fig. 2. The 20ps laser pulse is fed to three different lengths of step-index fiber for control of pulse dispersion to generate widths of ≈ 150ps, 1.2ns, and 2.5ns. As the pulse propagates, modal dispersion causes temporal broadening proportional to fiber length. To distinguish effects due to factors other than electron space charge at the crossover, we maintained constant energy in the input light. For this reason, when pulse width is increased, pulse intensity is reduced proportionately by use of N.D. filters. The pulse width measurements were made with the photo diode and the average power was measured with the radiometer. The peak power and energy per pulse were calculated. The available energy was about 1 nJ.

The cone angle of the light emitted from the exit end of the fiber varied with fiber length. The intensity uniformity also varied. Shorter lengths showed random-mottled interference modes, while the longest length produced a more nearly uniform spot with concentric interference rings. The SITV photocathode was was masked so that only the central 80-mm^2 area was illuminated. This gave fairly uniform intensity distribution from all three fibers.

The SITV accelerating voltage, which controls electronic gain and electron velocity, was held constant at the nominal (half of full gain) 6.5 kV. A variation in either parameter would influence the focus test. The tests were taken with the SITV in the non-gated mode. The 150ps pulse was filtered to operate the SITV at 25% of saturation level. The SITV was filtered and the CTF was measured. Then, without refocusing, we increased the laser pulse width to 1.2 ns and the CTF measurements were retaken. These data shown in Fig. 3 revealed no extreme defocusing. Similar measurements were made using a larger area pattern, and the 2.5 ns light pulse. This was done to illuminate most of the full 491 mm^2 of the photocathode with sufficient input intensity to operate near saturation. This provided the worst-case condition for stable focus. No degradation was observed.

TABLE II. Comparative responses of MCPTs and SITVs.

TUBE TYPE	OPTICAL GATE TIME (ns)				RESOLUTION (% of dc response)		SHUTTER RATIO		DYNAMIC* RANGE
	TURN ON	FULLY ON	TURN-OFF	TOTAL	4.5 lp/mm	8.0 lp/mm	photons	electrons	
MCPT	($t_{iris-on}$)	(iris closed)	($t_{iris-off}$)						
18 mm diameter	1.0 ± 0.5	1 - 2.5	0.6 ± 0.2	2.6-4.8	≈ 40	5 - 10	opaque	$>10^6$	~ 100-1000 for Sb_2S_3 tgt
25 mm diameter	1.7 ± 0.5	2.5 - 5.0	1.0 ± 0.2	4.9-9.0					~ 50-100 for silicon tgt
SITV	(t_r)	(peak)	(t_f)						
18 mm diameter	0.1 ± 0.05	0.5 - 1.0	0.1 ± 0.05	0.4 - 1.3	≈ 75	40 - 50	~ 10^5	10^3 - 10^4	~ 50-100
25 mm diameter	0.2 ± 0.1	0.7 - 2.0	0.2 ± 0.1	0.9 - 2.6					

*Vidicon dynamic range is a function of target charge and beam aperture. We have measured significant increases with large (>1-mil diameter) apertures.

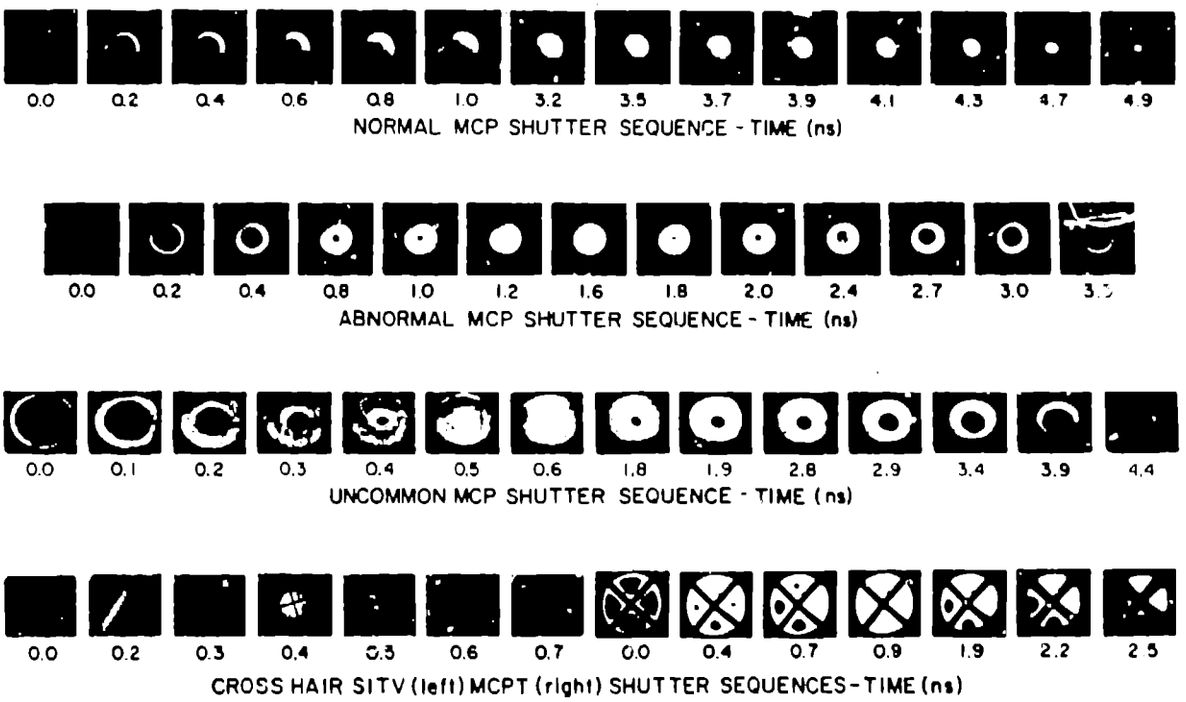

Fig. 1. Shutter sequences for MCPT's and SITV's. Zero is start of optical gate.

(b) Reciprocity: The same set up was used with a diaphram in place of the test pattern to measure SITV reciprocity. We obtained approximately equal signals from the three pulses as shown in Table III. The tests were repeated for an MCPT using extra fiber lengths to get more data points. A second photodiode was used to monitor phosphor intensity. The data are plotted in Fig. 4. These tests show that in this time range both tubes are essentially rate insensitive i.e., their response is proportional to the total optical energy deposited on the photocathode and not to the rate at which the energy was deposited.

Table III. SITV reciprocity Data

Pulse Width (ns)	Power/Pulse (W)	SITV Signal (μA)
0.15	7.34	1.
1.2	0.92	1.0
2.5	0.39	0.9

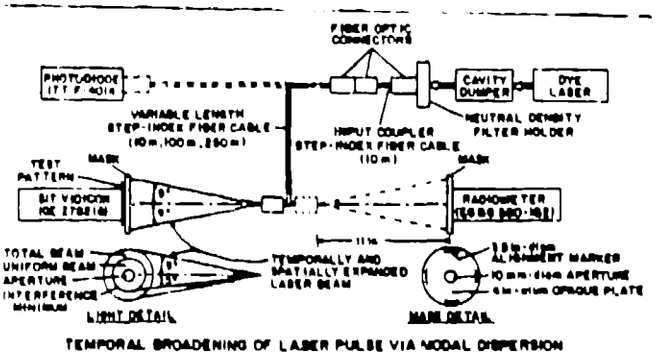

Fig. 2. The system used for the defocusing and reciprocity tests.

Fig. 3. SITV image focus vs light width. The results are shown for 150ps (top) and 1.2 ns (bottom), respectively. The line scans are through group 2, element 2 (4.5 lp/mm) and group 3, element 1 (8 lp/mm).

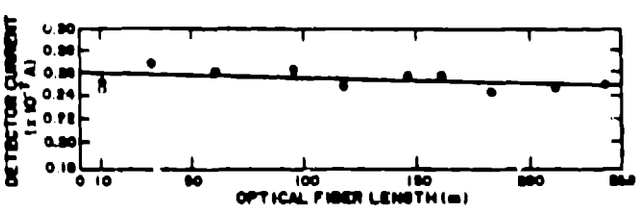

Fig. 4. MCPT reciprocity data. The 10-m, 100-m, and 250-m lengths correspond to the 150 ps, 1.2 ns, and 2.5 ns light widths.

V. Dynamic Shutter Ratio

The shutter ratios (for SITVs) shown in Table II were measured by first obtaining a given signal amplitude in the gated mode for a known optical intensity. Then the shutter tube was operated in the non gated mode and the intensity attenuated until the same signal amplitude was obtained. The ratio of the two intensities (corrected for differences in gain for the gated and non gated modes) is the shutter ratio. Recently, for two MCPTs, a more rigorous measurement was made which mapped the transmission behavior immediately before and after optical gate termination. The setup for this experiment is in Fig. 5. A PAR model LN-102 dye laser excited by a PAR model LN-100 nitrogen laser emits 500ps FWHM pulsed light which travels over an optical path of about 10 meters in air. The dye used was C481 with a peak wavelength of 480 nm. A long focal length lens focused the laser beam on the photocathode of an MCPT. Scattered light from this lens was used to saturate an RCA 8570 photo multiplier which triggered the gate pulser through an adjustable cable delay. The gate pulse (and therefore the MCPT optical gate) was adjustable from several tens of ns after to about 2 ns before the light pulse. First, the delay was adjusted so that the light pulse was coincident with the peak of optical gate and ND filters were inserted in the beam path until a minimum detectable signal was observed. The delay was then varied, "walking" the optical gate either side of the light pulse and ND filters were removed until the minimum detectable signal was again observed. In this manner the optical power extinction ratio of the MCPT was measured at several points in time relative to the peak of the optical gate. The data for one ITT and one VARO MCPT are plotted in Fig. 6. A long fluorescence tail (tens of ns duration at $\approx 10^{-6}$ of peak intensity) was associated with the main dye pulse and is shown at the leading edge of the optical gates. In the standard procedure for characterizing gating speed [1-3] only the top two decades of extinction are observable. Based upon that method, optical gate widths of $\approx$ 3ns would be determined for these MCPTS. However, for shuttering against light widths > optical gate widths, the dynamic shutter ratio must be included to accurately define the total gate function.

VI. Sector Gating

In this design, an electrically conductive cross-hair is deposited on the photocathode substrate before deposition of the S-20. The two radial strips are normal at their intersection in the center of the photocathode and their ends are connected at the photocathode perimeter by a circular metallic conductive ring. This produces four pie-shaped quadrants as shown in Fig. 7. The strip geometry and opacity is different for both tubes. The SITV design uses 5-mil wide aluminum oxide strips of $\approx 12\Omega$ dc resistance per radial leg with $\approx$ 50% transmission. The MCPT design uses 60-mil wide inconel strips with close to zero transmission (resistance not measured). The low resistance strips, although not designed to impedance match subnanosecond risetime pulses with the gate interface do provide the means for rapid propagation of gate voltages to the center of the photocathode. Because the area of each quadrant is approximately 1/4 the area of the non-segmented surface, the gating speed for the total surface should be increased $\sim$ 4x because all four quadrants turn on nearly simultaneously.

Sector-gating is best recognized if one sees full area behavior for non-segmented units repeated in each quadrant for the segmented unit. The shutter sequence (Fig. 2) for a fully illuminated cross-hair SITV shows no iris during turn-on or turn-off. In Fig. 8 we concentrated the light in individual quadrants and looked for irising near turn-off by successively re-imaging the laser. The fact that no iris was observed may be due to the gate-to-laser jitter, $\approx$ 50ps for the laser-linac system [7]. We estimate that electrical gates $\sim$ 250ps are required to see the impulse response with expected iris closure times of the order of tens of ps. These conditions may "blur" the time resolution sufficiently to mask any iris effects.

Sector-based irising in cross-hair MCPTS was observed as seen in Fig. 1. Photocathode processing for three F4111 MCPTs was monitored to assure repeatability of sheet resistance (or at least knowledge of the absolute values of resistance) for one segmented unit and two non-segmented units. One MCPT had cross-hairs on the photocathode only, a second had cross-hairs on both the photocathode and the MCP input surfaces. The non-segmented unit, to be used as a "control" sample to measure gains in gating speed from segmenting, failed (couldn't be gated off) so this test was inconclusive. Analysis of gating speeds for the two segmented units show essentially the same total gate times as those for typical non-segmented units. However, the simultaneous gating observed in each of the quadrants is encouraging and this experiment is being repeated with two new MCPTs, one nonsegmented, one with three sectors.

Intensity profiles for cross hair MCPTs showed highest transmission near both the apexes of quadrants two and four. In Fig. 9 profiles along three paths through the vertices of quadrant two verify the higher transmission in areas nearest the cross hair intercepts. The extent of this problem is being studied.

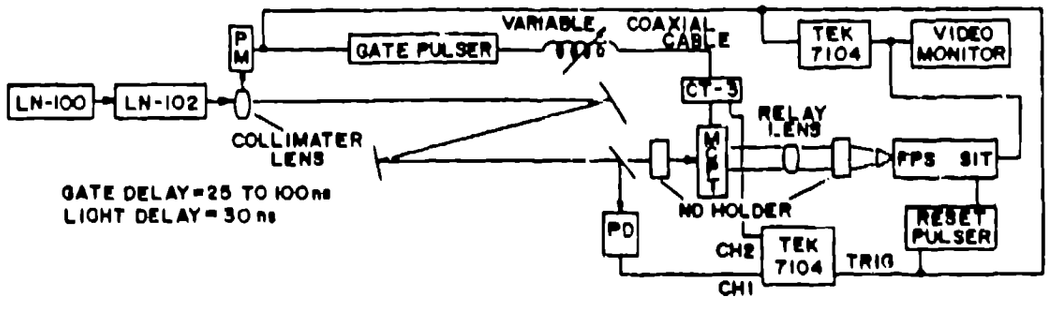

Fig. 5. The dynamic shutter ratio experimental setup.

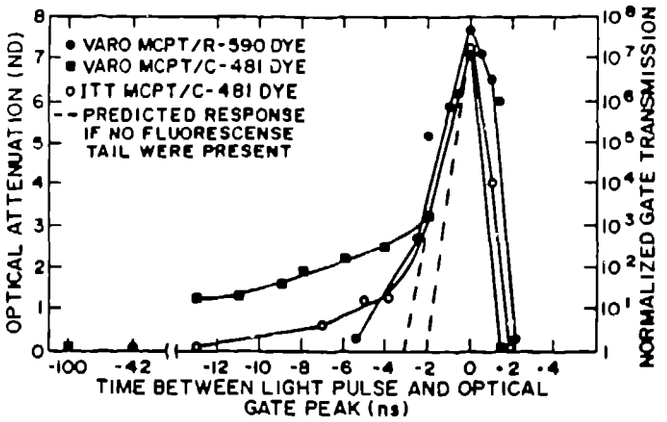

Fig. 6. Shutter ratio relative to center of optical gate. Zero is center of the gate

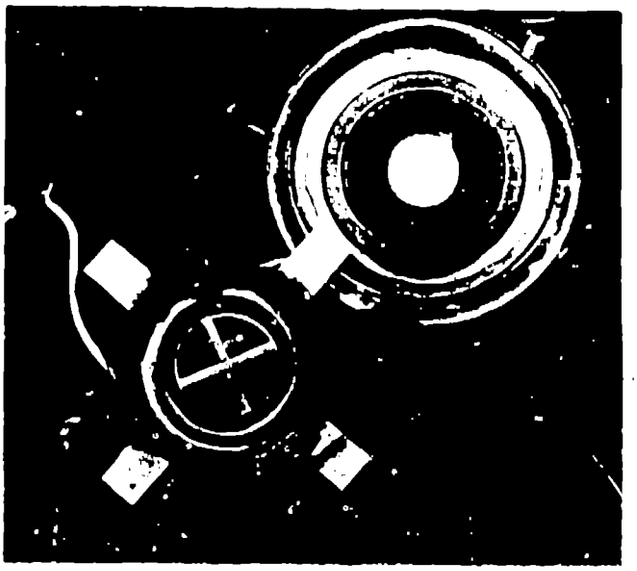

Fig. 7. SITV (top) and MCPT (bottom) with segmented photocathodes.

Optical transmission at indicated locations at PK+400ps.

Fig. 8. Iris-free response for SITV SN-C1937

VII. Infrared Stimulation for Improved Photoconductivity

Using infra red light to improve gating speed by increasing photocathode conductivity during the optical gate was explored. The bandgap for S-20 is ≈ 1eV and the photoelectric emission threshhold is ≈ 1.5eV[8]. To excite valence electrons across the bandgap into the conduction band without inducing photoemission requires radiation > 1eV (1240nm) and < 1.5 eV (830nm). A simple expression was developed [9] to estimate (1) the required carrier concentrations and lifetimes to produce a discernable reduction in S-20 sheet resistance and (2) the required optical energy to produce the excitation.

Our first experiment used a Xenon flash (filtered to transmit all wavelengths > 830nm) of about 2μs width that produced ≈ 250 W/cm^2 at the MCPT photocathode. The total optical energy available for excitation was ≈ 0.5mJ. The excitation pulse was time-phased to overlap a much narrower (180 ps FWHM) light from an 820nm pulsed laser diode used to measure the optical gate width. The excitation energy during gate time was ≈ 0.5μJ. No increases in gating speed were observed.

Our second experiment, shown in Fig. 10, used a Q-switched Nd:YAG laser (1060nm, ≈ 70ns FWHM, 160PPS) for excitation and a dye laser [1,2] (650nm, ≈ 20ps FWHM, 160PPS) for the visible source. Both lasers and the gate generator were synchronized and phased to center the gate and visible pulses within the excitation pulse. The YAG peak power incident on the full 491 mm^2 of the photocathode was 470 watts. This provided ≈ 33μJ total with again ≈ 0.5μJ during gate time but with mono-energetic photons (1.17eV). This excitation did not improve gating speed. We then concentrated the YAG light in a spot ≈ 5-mm-diameter producing power density ≈ 24 W/mm^2.

The phasing between the dye laser and the electrical gate was adjusted to "freeze" the optical gate in its turn-on phase where irising was visible (Fig. 11). The YAG light was positioned to intercept the edge of the iris where we expected to see bulges corresponding to increased gate voltage propagation velocity induced by the infrared illumination. No pertubations were observed in the iris indicating negligible photo-induced conductivity. With the latter excitation our calculations [10] show that if the product of carrier mobility and lifetime were $\geq 2.5\times10^{-9}$cm^2/volt an increase in iris propagation rate should have been observed.

IX. Gate Driving Techniques

Several gate pulsers and pulse injection methods were described in earlier work [7]. To date, the fundamental limitation has been in properly matching the gate generator with the gate interface. Consequently, excessive ringing and pulse width dispersion result when the two are electrically connected and driven with

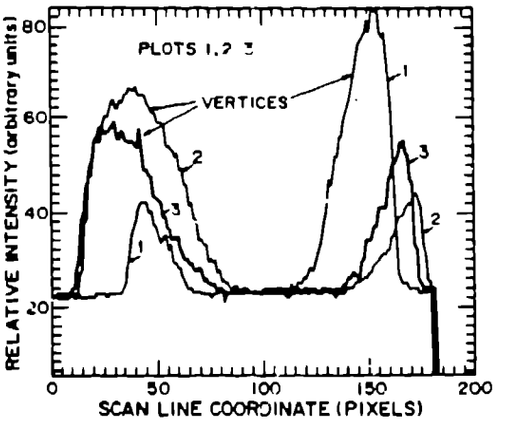

Fig. 9. Intensity profiles through vertices of quadrant two of MCPT SN-14-992-4.

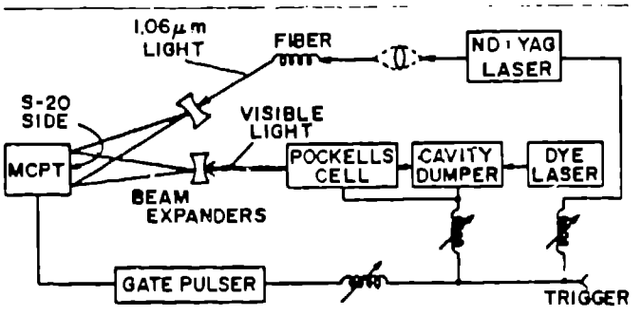

Fig. 10. Setup for the infrared stimulation studies.

Fig. 11. Optical gate for MCPT SN-725/6 at 200ps prior to fully-on phase. Part a shows iris detail, b shows location of infrared excitation pulse.

short risetime (100ps to 1ns) pulses. To a first approximation, the gate interface is a capacitor that does not terminate any transmission line properly. It is a "matched" load only at $\omega = (1/C)|Z_o|$ where Z_o is the characteristic impedance of the line. For 25-mm-diameter SITVs (C ≈ 3.5pf) driven with Gaussian pulse of ≈ 100ps risetime, $|Z_o| \approx 13\Omega$. For each sector in a 4 quadrant tube $|Z_o| \approx 3.25\Omega$.

We are currently testing high frequency 50:12.5Ω impedance tranformers made by Avtech. Preliminary test results show that a 150-ps-wide pulse on the primary is widened to 300ps on the secondary. The small signal (≈ 2V on primary, 1V on secondary) and large signal (≈ 200V as primary, 100V on secondary) responses are identical, showing no saturation effects at the higher voltages. These are to be used as single point drivers for SITVs or multipoint for the higher impedance MCPTs.

For multipoint driving of segmented SITVs we have used matched power dividers to split the line into n parallel 50-Ω lines (each driving the tube) such that $50/n \approx |Z_o|$. The current version of this network where n=12, for $|Z_o| \approx 4.2\Omega$ has been tested using a TDR. The best risetime obtained is 300 ps.

Acknowledgements

The authors thank James Schoenborn, EG&G Santa Barbara Operations for help in the sector-gated and dynamic shutter ratio measurements, Joseph Calligan III, EG&G Los Alamos Operations for help in design and evaluation of multipoint driving networks, and Teresa Martinez, EG&G Los Alamos Operations for help in data analysis and image enhancement.

References

[1] N.S.P. King, et al., "Nanosecond gating properties of proximity-focused microchannel-plate image intensifiers," Proceedings SPIE, vol. 288, pp. 425-433, 1981.

[2] G.J. Yates, et al., "Image shutters: gated proximity-focused microchannel-plate (MCP) wafer tubes vs gated silicon intensified target (SIT) vidicons," Proceedings SPIE, vol. 348, pp. 422-433, 1982.

[3] G.J. Yates, et al., "A high resolution SIT (silicon-intensified-target) TV tube for subnanosecond image shuttering," Los Alamos National Laboratory Report, LA-9771-MS, expected publication Dec. 1983.

[4] J.L. Datch, Jr. and J.W. Ogle," A distributed RC radial transmission line theory applied to the gain characteristics of gated microchannel-plate image intensifiers," EG&G Report, EG&G 1183-2404, 1980.

[5] J.L. Datch, Jr. and B.W. Noel, "Radial pulse propagation and impedance characteristics of optically shuttered channel intensifier tubes," Proceedings SPIE, vol. 288, pp. 434-446, 1981.

[6] C.K. Hinrichs, et al., "Photocathode development," EG&G Report, EG&G 1183-1846, pp. 80-83, 1982.

[7] G.J. Yates, et al., "Overview of pulsers for nanosecond gating of image shutter tubes," Proceedings SPIE, vol. 348, pp. 434-437, 1982.

[8] L. Biberman and S. Nudelmand, eds., photoelectron imaging devices, vol. 1, Plenum Press, New York, 1971, pp. 161-175.

[9] P.L. Gobby et al., "Using photoconductivity to improve image tube gating speeds," this symposium.